

Robust spin polarization of Yu-Shiba-Rusinov states in superconductor/ferromagnetic insulator heterostructures

A. Skurativska^{1,*}, J. Ortuzar², D. Bercioux^{1,3}, F. S. Bergeret^{1,4,†} and M. A. Cazalilla^{1,3,‡}

¹*Donostia International Physics Center, 20018 Donostia–San Sebastián, Spain*

²*CIC nanoGUNE-BRTA, 20018 Donostia–San Sebastián, Spain*

³*IKERBASQUE, Basque Foundation for Science, Plaza Euskadi 5, 48009 Bilbao, Spain*

⁴*Centro de Física de Materiales (CFM-MPC), Centro Mixto CSIC-UPV/EHU, 20018 Donostia–San Sebastián, Spain*



(Received 2 March 2023; revised 9 May 2023; accepted 11 May 2023; published 15 June 2023)

Yu-Shiba-Rusinov (YSR) states arise as subgap excitations of a magnetic impurity in a superconducting host. Taking into account the quantum nature of the impurity spin in a single-site approximation, we study the spectral properties of the YSR excitations of a system of magnetic impurity in a spin-split superconductor, i.e., a superconductor in proximity to a ferromagnetic insulator at zero external magnetic fields. The YSR excitations of this system exhibit a robust spin polarization that is protected from fluctuations and environmental noise by the exchange field of the ferromagnetic insulator, which can be as large as a few Tesla. We compare the results of this quantum approach to the classical approach, which conventionally predicts fully polarized YSR excitations even in the absence of exchange and external magnetic field. Turning on a small magnetic field, we show the latter splits the YSR excitations in the regime where the impurity is strongly coupled to the superconductor, whilst the classical approach predicts no such splitting. The studied system can potentially be realized in a tunnel junction connected to a quantum dot in proximity to a spin-split superconductor.

DOI: [10.1103/PhysRevB.107.224507](https://doi.org/10.1103/PhysRevB.107.224507)

I. INTRODUCTION

Magnetic impurities in superconductors often feature Yu-Shiba-Rusinov (YSR) excitations. These subgap bound states arise due to the exchange coupling between the impurity and the superconductor [1–3]. Much of the recent effort devoted to the study of these excitations is driven by experimental advances in scanning tunneling spectroscopy, which allow one to access the spectral properties of YSR excitations with atomic-scale resolution [4–6]. For example, from the spectrum and spatial dependence of the YSR excitations, we can learn about nonconventional pairing properties or the symmetry of the Fermi surface of the host superconductor [7–9]. In addition to magnetic impurities on the surface of superconductors, the YSR excitations have also been investigated in superconducting devices with molecular junctions [10] as well as quantum dots with superconducting leads [11–16].

In many theoretical treatments, including the pioneering works of Yu, Shiba, and Rusinov, magnetic impurities are modeled as classical spins (see, e.g., Ref. [17] for a review). Thus, the impurity is described as an external scattering potential for the quasiparticles of the superconductor. The potential has an opposite sign for opposite spin orientation along the spin-quantization axis, leading to the two nondegenerate in-gap YSR excitations with opposite energy and full spin polarization. For this reason,

systems with the YSR excitations are often proposed as ideal platforms for superconducting spintronics and magnetic characterization at the microscopic scale [18–20]. However, this description often overlooks the quantum nature of the spin degree of freedom of magnetic atoms, molecules, or quantum dots [13,21–25]. Indeed, quantum (and thermal or noise) fluctuations destroy the spin polarization of the YSR excitations. Spin polarization can be restored by applying external magnetic fields [26,27]. However, magnetic fields applied to superconducting devices also have unwanted orbital effects, which may induce supercurrents and suppress superconductivity.

In this paper, we propose using a ferromagnetic insulator (FMI) adjacent to the superconductor to induce a finite spin polarization of the YSR excitations. The FMI leads to an effective exchange field of strength h in the superconductor in the absence of external magnetic field [28–31]. The exchange field is induced by the magnetic proximity effect at the FMI/superconductor interface [32,33], and leads to a spin splitting equivalent to that of a magnetic field as large as tens of Tesla without any orbital effects. To account for quantum fluctuations in the spectrum of a magnetic impurity coupled to such a spin-split superconductor, we extend the single-site model used in Refs. [24,34,35]. This approach provides an excellent qualitative description of the spectra obtained experimentally [35]. It also captures the properties of the ground state and low lying states of the system while being computationally cheaper than the numerical renormalization group (NRG) [27,36]. We demonstrate that the exchange field h induced by the FMI suppresses fluctuations and leads to a finite spin polarization of the YSR excitations without

*anastasiia.skurativska@dipc.org

†fs.bergeret@csic.es

‡miguel.cazalilla@dipc.org

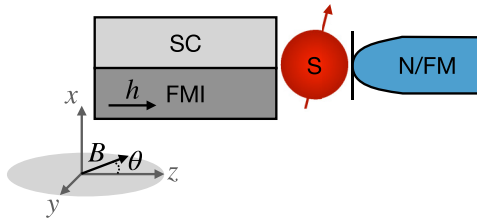


FIG. 1. Schematic picture of a possible realization of the studied system. It consists of a superconductor in proximity to a ferromagnetic insulator coupled to a quantum dot or a molecule that can be modeled as a spin- S quantum impurity. The right normal metal is a ferromagnetic tunneling contact to probe the spin polarization. An external magnetic field \mathbf{B} is applied in different directions.

introducing any spin splitting of the latter. In addition, if a small external magnetic field is applied, we show that the YSR excitations split only if the system is in the regime where the impurity spin is strongly coupled to the superconductor. In contrast, as we also show below, the classical description of the impurity yields no such spin splitting of the YSR excitations, the main effect of the external magnetic field being a shift of the energy of the YSR peaks in the spectral function.

For the sake of simplicity, we focus our analysis on a spin- $\frac{1}{2}$ impurity and isotropic exchange coupling between the superconductor and the magnetic impurity. The latter may correspond, for example, to a quantum dot coupled to an FMI/superconductor system (see Fig. 1), which can be realized in superconductor/semiconducting nanowire heterostructures in proximity to a FMI [37]. For other setups relevant to magnetic atoms or molecules on the surface of superconductors, our results can be straightforwardly extended to account for larger impurity spins, single-ion anisotropy, as well as anisotropic exchange [24,35]. The remaining sections of this paper are organized as follows: In the next section, we introduce the model and describe the many-body spectrum of the FMI/superconductor–quantum dot system as a function of the exchange coupling, the exchange field, and the external magnetic field. In Sec. III, we discuss the spectral properties of the YSR excitations focusing on spin polarization. Finally, we present our conclusions in Sec. IV. Appendix A contains the details of the classical solution of the model. In Appendix B, we provide the details of the analysis of the spin polarization described in Sec. III.

II. MODEL AND MANY-BODY SPECTRUM

We consider a magnetic impurity in a spin-split superconductor as schematically shown in Fig. 1. The exchange field h of the device is achieved by bringing a conventional (s -wave) superconductor in proximity to a FMI. Assuming that the thickness of the superconductor is smaller than the superconducting coherence length, it is a good approximation to consider a homogeneous exchange field h [31]. Thus, the Hamiltonian of the system reads

$$H = H_0 + H_J + H_B, \quad (1)$$

where

$$H_0 = \sum_{\mathbf{k}, \sigma} \xi_{\mathbf{k}} c_{\mathbf{k}, \sigma}^\dagger c_{\mathbf{k}, \sigma} + \Delta \sum_{\mathbf{k}} (c_{\mathbf{k}, \uparrow}^\dagger c_{-\mathbf{k}, \downarrow}^\dagger + \text{H.c.}) - h \sum_{\mathbf{k}} (c_{\mathbf{k}, \uparrow}^\dagger c_{\mathbf{k}, \uparrow} - c_{\mathbf{k}, \downarrow}^\dagger c_{\mathbf{k}, \downarrow}), \quad (2a)$$

$$H_J = J \sum_{\mathbf{k}, \sigma \sigma'} c_{\mathbf{k}, \sigma}^\dagger \mathbf{S} \cdot \mathbf{s}_{\sigma \sigma'} c_{\mathbf{k}, \sigma'}, \quad (2b)$$

$$H_B = \mathbf{B} \cdot \mathbf{S}. \quad (2c)$$

Here, H_0 describes a superconductor with mean-field pairing potential of strength Δ and an exchange field $\mathbf{h} = h\mathbf{e}_z$ along the z axis; H_J is the isotropic exchange interaction between the host superconductor and the magnetic impurity described by the spin operator \mathbf{S} with coupling strength J . Finally, H_B accounts for the Zeeman energy due to an external magnetic field $\mathbf{B} = B(\cos \theta, \sin \theta)$ where the angle θ (see Fig. 1) measures the tilt between the magnetic field and the z axis.

In Eq. (2), the operator $c_{\mathbf{k}, \sigma}^\dagger (c_{\mathbf{k}, \sigma})$ creates (annihilates) an electron with the momentum \mathbf{k} , the spin state $\sigma \in \{\uparrow, \downarrow\}$, and the electron dispersion (measured from the chemical potential) $\xi_{\mathbf{k}}$, \mathbf{s} being the Pauli matrices $\mathbf{s} = (s^x, s^y, s^z)$. We assume an external magnetic field $|\mathbf{B}| \ll |h|$. In the case of thin films or wires, as considered here, the orbital effect of an external in-plane magnetic field is negligibly small, while its coupling to the impurity spin persists. As we discuss below, it can be used as an additional probe into the properties of the YSR excitations.

Furthermore, let us point out that the range of Zeeman couplings analyzed in this paper is different from the regime previously studied in Refs. [14,27]. References [14,27] consider a system of a quantum dot coupled to a superconductor in the regime when the external magnetic field couples to both a superconductor and a quantum dot.

To solve the model in Eq. (1) we use two different approaches. On the one hand, we use a single-site model in which the superconducting host is effectively modeled by a single site but its coupling to the impurity spin is described exactly by treating \mathbf{S} as spin- $\frac{1}{2}$ operator. On the other hand, we use the classical description in which the superconductor is treated as an extended system but the exchange coupling is simplified by treating the impurity spin \mathbf{S} as a classical vector.

In the single-site model, we simplify the Hamiltonian H describing the system (2) to the following model:

$$H_0 = \Delta (c_{\uparrow}^\dagger c_{\downarrow}^\dagger + \text{H.c.}) - h (c_{\uparrow}^\dagger c_{\uparrow} - c_{\downarrow}^\dagger c_{\downarrow}), \quad (3a)$$

$$H_J = J \sum_{\sigma \sigma'} c_{\sigma}^\dagger \mathbf{S} \cdot \mathbf{s}_{\sigma \sigma'} c_{\sigma'}, \quad (3b)$$

$$H_B = \mathbf{B} \cdot \mathbf{S}. \quad (3c)$$

This model is an extension of the single-site model introduced in Refs. [24,34], which takes into account the exchange field h due to proximity to the FMI as well as the external magnetic field \mathbf{B} [38]. Within the single-site model and for a spin- $\frac{1}{2}$ impurity, the Hilbert space of the model in Eq. (1) is the tensor product of the four-dimensional Hilbert space of the single superconductor site and the two-dimensional Hilbert space of the impurity spin: $\mathcal{H} = \{(|0\rangle, |\uparrow\downarrow\rangle \equiv |2\rangle, |\uparrow\rangle, |\downarrow\rangle) \otimes (|\pm \frac{1}{2}\rangle)\}$, where we have defined $|\sigma\rangle = \{|\uparrow\rangle, |\downarrow\rangle\} = c_{\sigma}^\dagger |0\rangle$ and

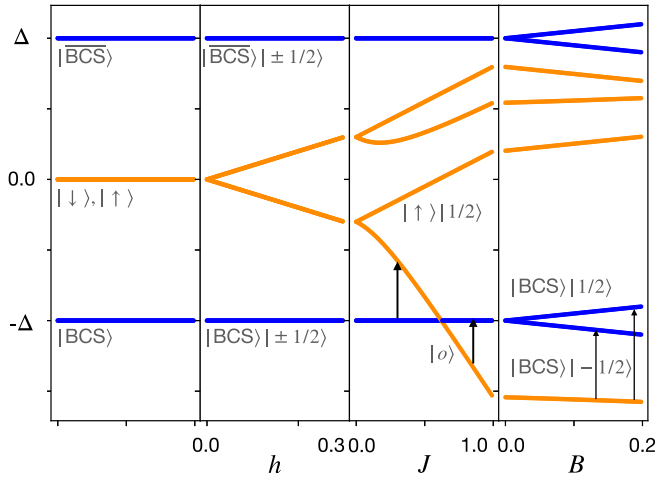


FIG. 2. Evolution of the many-body spectrum of the single-site model in Eq. (1) as the exchange field (h), exchange coupling (J), and external magnetic field (B) are switched on sequentially. Their values are given in units of the strength of the superconducting pairing potential Δ . The energies of the even and odd fermion-parity states are shown in blue and orange color, respectively. The expression for the odd-parity eigenstate $|o\rangle$ is given in Eq. (4). The arrows indicate the subgap transitions corresponding to the YSR excitations with and without B . In the rightmost panel, the system is in the strong coupling regime and the YSR excitations are split by B .

$|o\rangle$ is the zero-particle state. The Hamiltonian conserves the fermion parity, which for the single-site model takes the form $\mathcal{P} = \prod_{\sigma} (-1)^{n_{\sigma}}$, where $n_{\sigma} = c_{\sigma}^{\dagger} c_{\sigma}$. Thus, all eigenstates can be labeled by their fermion parity and therefore the Hilbert space splits into the direct sum of the even- ($\mathcal{P} = +1$) and odd-parity ($\mathcal{P} = -1$) sectors, i.e., $\mathcal{H} = \mathcal{H}_e \oplus \mathcal{H}_o$ with $\mathcal{H}_e = \{(|\text{BCS}\rangle, |\overline{\text{BCS}}\rangle) \otimes (|\pm \frac{1}{2}\rangle)\}$ and $\mathcal{H}_o = \{(|\uparrow\rangle, |\downarrow\rangle) \otimes (|\pm \frac{1}{2}\rangle)\}$. Here we have introduced the notation $|\text{BCS}\rangle = \frac{1}{2}(|2\rangle + |0\rangle)$ and $|\overline{\text{BCS}}\rangle = \frac{1}{2}(|2\rangle - |0\rangle)$ for the eigenstates of H_0 with eigenvalues $-\Delta$ and Δ , respectively. The single quasiparticle excitations of the superconductor are denoted by $|\uparrow\rangle$ and $|\downarrow\rangle$ and have a zero eigenvalue of H_0 at $h = 0$.

Figure 2 shows the evolution of the many-body spectrum of the system as a function of the exchange field h , the coupling J , and the external magnetic field $\mathbf{B} = B\mathbf{e}_z$ as obtained from the exact diagonalization of the Hamiltonian (1) in the single-site approximation. The leftmost panel shows the spectrum of the Hamiltonian in Eq. (3a) with $h = 0$.

We next discuss the effect of different couplings as we add them sequentially. An exchange field h lifts the degeneracy of the quasiparticle states giving rise to two twofold odd-parity degenerate states $|\uparrow\rangle|\pm \frac{1}{2}\rangle$ and $|\downarrow\rangle|\pm \frac{1}{2}\rangle$ with energies $\pm h$. As we show below, this splitting in the presence of the magnetic exchange with the impurity leads to the nonzero polarization of the YSR excitations. The exchange interaction H_J entangles the impurity doublet $|\pm \frac{1}{2}\rangle$ with the odd-parity states of the superconductor, resulting in a further splitting of the many-body states.

However, in the weak coupling regime, i.e., for small values of J compared to Δ , the ground state of the system is in the even-parity sector, and it is the tensor product of the impurity spin doublet and the BCS ground state $|\text{BCS}\rangle|\pm 1/2\rangle$. In

this regime, the system cannot gain much energy by coupling to the magnetic impurity, and therefore the electrons in the superconductor remain paired, leaving the impurity spin unscreened. Thus, the ground state is doubly degenerate, and the total spin projection of the ground state on \mathbf{e}_z is $S_T^z = \pm 1/2$. We shall refer to this ground state as a doublet and assume that the system is in a mixed state with equal probabilities of the two states of the doublet (this results in zero net polarization of the YSR at $h = 0$, as discussed in the following section). Applying a finite magnetic field B selects one of the states of the doublet (or a linear combination thereof) as the absolute ground state and induces a finite spin polarization, polarization which persists even at $h = 0$. However, for weak magnetic fields, we expect the latter not to be robust to thermal fluctuations and environmental noise. This robustness can be achieved with the help of the exchange field h induced in the superconductor by proximity to an FMI.

At sufficiently large J (strong coupling regime), the ground state becomes the odd-parity state with $S_T^z = 0$ resulting from the entanglement of the impurity doublet and one superconductor (spin-split) quasiparticle excitation, which is given by

$$|o\rangle = \frac{1}{\sqrt{1 + \gamma_0^2}} \left(|\downarrow\rangle \left| + \frac{1}{2} \right\rangle - \gamma_0 |\uparrow\rangle \left| - \frac{1}{2} \right\rangle \right), \quad (4)$$

where $\gamma_0 = (h + \sqrt{h^2 + J^2})/J$. Although the full spin rotation symmetry is broken by the exchange field induced by the FMI, below we shall often refer to this state as the singlet.

The state $|o\rangle$ becomes the ground state at a critical value of the exchange coupling $J_c = \frac{2}{3}(\sqrt{4\Delta^2 - 3h^2} - \Delta)$, at which the system undergoes a quantum phase transition (QPT). Across the QPT, the fermion parity \mathcal{P} of the ground state changes. Since the tunneling of a single electron (or hole) into the system changes the fermion parity, only excitations between states of opposite parity are accessible using tunneling probes. In particular, the YSR excitations are the lowest lying excitations and correspond to transitions between the ground states in different parity sectors (they are indicated by arrows in Fig. 2). In the weak coupling regime ($J < J_c$), the YSR excitation is a transition from the doublet ground state to the singlet state $|o\rangle$ given in Eq. (4). On the other hand, in the strong coupling regime ($J > J_c$), the YSR excitation corresponds to a transition from $|o\rangle$ to the doublet ground states in the even-parity sector.

When an external magnetic field \mathbf{B} is applied, it lifts the twofold degeneracy of the ground state in the even-parity sector. This results in the splitting of the YSR excitations *only* in the strong coupling regime. In the weak coupling regime, such splitting does not take place because, as explained above, the magnetic field selects one of the states of the even-parity doublet subspace as the absolute ground state. As we will discuss in Sec. III, one can regard the splitting of the YSR excitations as a consequence of the quantum nature of the impurity spin: Since the tunneling electron (hole) can bring back the superconductor from the singlet state $|o\rangle$ to the $|\text{BCS}\rangle$ state, the impurity spin is left unscreened and free to precess in the external magnetic field. Note that a classical spin would simply align in the direction of the external magnetic field (see discussion below and Appendix A).

Although it provides a fully quantum mechanical description of the coupling between the superconductor and the magnetic impurity, the single-site model described above does not capture many of the effects of the wide continuum scattering states of the superconductor. Therefore, as far as the spectral properties of the YSR excitations are concerned, the results are rather qualitative and the model is unable to provide information about, e.g., the spatial extent of the excitations.

Alternatively, the Hamiltonian in Eq. (2) can be simplified by modeling the magnetic impurity as a classical spin. Note that, in the case of a quantum impurity, the exchange coupling H_J contains a spin-flip term with nontrivial consequences, especially for impurities with low spin S . However, in the classical approach, the impurity spin is treated as a classical vector that aligns with the external magnetic field (when present), and therefore it can be parametrized as $\mathbf{S} = S(\cos\theta, \sin\theta)$, where θ is the angle subtended by the magnetic field \mathbf{B} and the exchange field $\mathbf{h} \propto \mathbf{e}_z$. This results in a localized spin-dependent scattering potential proportional to $JS(\cos\theta s_z + \sin\theta s_x)$ being added to the Bogoliubov–de Gennes (BdG) Hamiltonian describing the superconductor. We refer the reader to Appendix A, where we provide further details of the classical approach and describe how the subgap spectrum is obtained.

Notice the complementary character of the two approaches: Generally, the classical approximation provides a good description of impurities with a large spin, especially in the weak coupling regime. However, treating the impurity spin as a classical vector does not account for any quantum fluctuations that are important in the strong coupling regime, particularly for the impurity spin $\frac{1}{2}$. The single-site approximation captures the effect of quantum fluctuations in a minimal fashion and, in addition, allows us to take into account the effects of single-ion anisotropy and anisotropy in the exchange coupling.

In the following section, we will describe the effect of the exchange and applied magnetic fields on the spectral properties of the YSR excitations and compare the results obtained using the two approaches mentioned above. We will demonstrate that including the effect of the quantum fluctuations is crucial to correctly describe the spectral properties of the YSR states.

III. SPECTRAL PROPERTIES OF THE SUBGAP EXCITATIONS

In order to illustrate the consequences of treating the impurity spin quantum mechanically, we compare the spectral properties of the YSR excitations in the single-site and classical approaches. Besides the dependence of the excitation energy on the various system parameters, we are interested in their spin-polarization properties, which can be accessed experimentally using a spin-polarized tunneling probe [39]. As explained below, the spin polarization of the YSR excitations is defined as the difference of the spectral weight of the spin-up and spin-down YSR peaks of the spectral function measured using a tunneling probe (see Fig. 1). We normalize the polarization to the maximum of the sum of spectral weights for the two spin orientations of each YSR excitation.

Let us briefly recall how the polarization can be measured using a tunneling probe. In the tunneling regime, the full Hamiltonian describing the tunneling of electrons (or holes) from a tunneling probe contains three terms:

$$H_{\text{tot}} = H + H_t + H_{ts}, \quad (5)$$

where H is the system Hamiltonian, which we describe using the single-site model from Eq. (3); the Hamiltonian for the (spin-polarized) tunneling probe is denoted H_t , which is expressed in terms of the creation (annihilation) operators of the electrons in the probe, i.e., d_σ^\dagger (d_σ); and the tunneling Hamiltonian is denoted H_{ts} . For a quantum impurity in the Kondo regime, H_{ts} reads (see, e.g., Ref. [40])

$$H_{ts} = T_0 \sum_{\sigma} c_{\sigma}^{\dagger} d_{\sigma} + T_1 \sum_{\sigma, \sigma'} c_{\sigma}^{\dagger} \mathbf{S} \cdot \boldsymbol{\sigma}_{\sigma\sigma'} d_{\sigma'}, \quad (6)$$

where T_0 is the direct tunneling amplitude into the superconductor and T_1 is the tunneling amplitude through the magnetic impurity. Notice that the system operators appearing in T_0 (e.g., c_{\uparrow}^{\dagger} , for $\sigma = \uparrow$) and T_1 (e.g., $c_{\downarrow}^{\dagger} S^+ + c_{\uparrow}^{\dagger} S^z$, for $\sigma = \uparrow$) when acting upon a given state invert its fermion parity and change S_T^z by $\pm \frac{1}{2}$. Thus, for zero external magnetic field B , the contributions to the normal current in the weak tunneling regime [41] are of the order $|T_0|^2$ and $|T_1|^2$. Furthermore, when the magnetic field \mathbf{B} is not aligned with the exchange field $\mathbf{h} \propto \mathbf{e}_z$, S_T^z is not a good quantum number and there is also an interference term proportional to $|T_0^* T_1| \sim B$. However, for the small magnetic fields considered here, we shall neglect this correction. In addition, since the single-site model only provides a *qualitative* description of the spectral amplitudes, below we focus on the $|T_0|^2$ contribution to the tunneling current only. Indeed, since the involved operators obey the same selection rules, the $|T_1|^2$ contribution results from transitions between the same many-body states and simply yields an additional (positive) contribution to the current. Focusing on the $|T_0|^2$ contribution and using the standard tunneling formalism [41], the spin-polarized tunneling current is determined by the spin-resolved spectral function $A_{\sigma}(\omega)$, which is obtained from the imaginary part of the local Green's function (GF), $A_{\sigma}(\omega) = -\text{Im}[G_{\sigma}^R(\omega)]/\pi$, where $G_{\sigma}^R(\omega)$ is the Fourier transform of

$$G_{\sigma}^R(t) = -i\theta(t)\langle\{c_{\sigma}(t), c_{\sigma}^{\dagger}(0)\}\rangle. \quad (7)$$

Hence, for $\omega > 0$, the spectral function takes the form [42]

$$A_{\sigma}(\omega) = \sum_n |\langle\psi_n|c_{\sigma}^{\dagger}|\psi_0\rangle|^2 \delta(\omega - \epsilon_n + \epsilon_0). \quad (8)$$

Below, we focus on the YSR excitations which correspond to transitions from the ground state of the system, $|\psi_0\rangle$, to the lowest lying excited state $|\psi_1\rangle$ (or states for $B \neq 0$ and $J > J_c$; see below). The spectral weight of the YSR excitations is thus given by

$$Z_{\sigma} = |\langle\psi_1|c_{\sigma}^{\dagger}|\psi_0\rangle|^2. \quad (9)$$

Hence, we define a (normalized) polarization spectral function for the YSR excitations as follows:

$$P(\omega) = \left(\frac{Z_{\uparrow} - Z_{\downarrow}}{Z_{\uparrow} + Z_{\downarrow}}\right) \delta(\omega - \epsilon_1 + \epsilon_0), \quad (10)$$

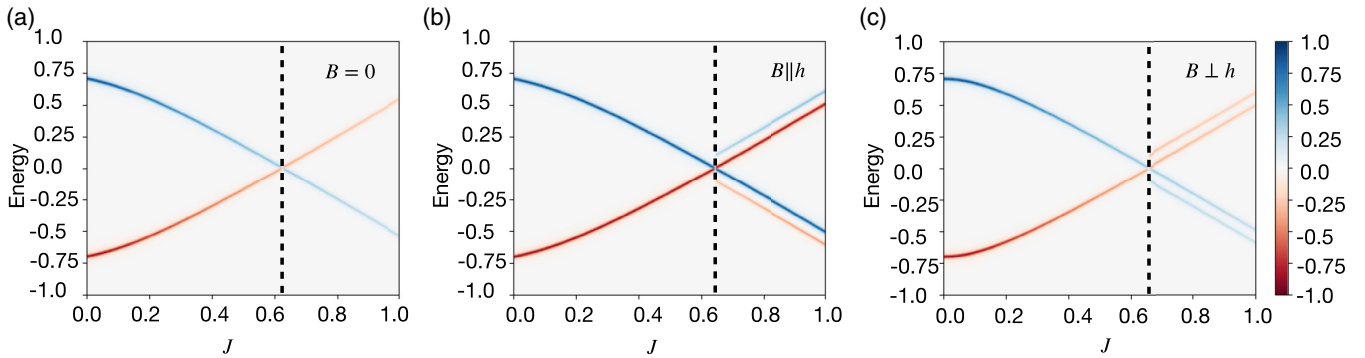


FIG. 3. Spin polarization of the YSR excitations as a function of the energy E and the exchange coupling J in the single-site model. In the absence of the magnetic field, the system shows no splitting of the YSR excitations (a), while adding the magnetic field gives rise to the splitting of the YSR excitations in the strong coupling regime (b, c). The dashed line indicates the QPT. All the energies are given in units of Δ . The values of the parameters used to generate the plots are $B = 0.1$ and $h = 0.3$. Notice that the value of the B field considered here is exaggerated in order to make the splitting visible on the scale of the plot.

where the maximum in the normalization corresponds to the sum of the spectral weights with spin-up and spin-down YSR excitations. For $B \neq 0$, the above expressions must be generalized to include all the relevant low lying states involved in the YSR excitation (see Fig. 2). Further details of the calculations in the single-site approach are relegated to Appendix B. For the classical approach, the polarization of the YSR excitations is obtained by extending the scattering solution of Yu, Shiba, and Rusinov [1–3] to take into account the exchange field h , with the details of these calculations being provided in Appendix A. Below, we will compare the above polarization spectral function to the results of the normalized polarization obtained from the classical approach.

However, before fully discussing the results of those calculations, let us clarify a subtle issue regarding the calculation of the polarization of the YSR excitations in the single-site approach. Let us recall that, in the weak coupling regime at zero magnetic field, the ground state of the system is the doublet $|e_{\pm}\rangle = |\text{BCS}\rangle \pm \frac{1}{2}$. An unbiased preparation of the system will result in the ground state being either $|e_{+}\rangle$ or $|e_{-}\rangle$ with equal probability, which is described by the following mixed state:

$$\rho_e = \frac{1}{2}(|e_{+}\rangle\langle e_{+}| + |e_{-}\rangle\langle e_{-}|). \quad (11)$$

In this expression, the prefactor $p_{i=\pm} = \frac{1}{2}$ refers to the classical probability for the system to be found in one of the states of the doublet. Therefore, the expression for the spectral function needs to be modified in order to take into account that the ground state is a mixed state, which results in the following expression:

$$A_{\sigma}(\omega) = \sum_{i=\pm} p_i \sum_n |\langle \psi_n | c_{\sigma}^{\dagger} | e_i \rangle|^2 \delta(\omega - \epsilon_n + \epsilon_0). \quad (12)$$

Note that, in the absence of the exchange and external magnetic fields (i.e., $h = B = 0$), a tunneling electron (hole) will induce a transition to a state that has a nonzero overlap with the lowest-energy odd-parity state:

$$|o\rangle = \frac{1}{\sqrt{2}} \left(\left| \downarrow \right\rangle + \frac{1}{2} \left| \uparrow \right\rangle - \left| \uparrow \right\rangle - \frac{1}{2} \right). \quad (13)$$

This yields equal spectral weight of the YSR excitation for the two spin orientations, i.e., $Z_{\uparrow} = Z_{\downarrow} = \frac{1}{16}$, hence resulting in zero spin polarization. Zero polarization is also obtained when the calculation is carried out in the strong coupling regime, in which the ground state is a pure state corresponding to the odd-parity singlet $|o\rangle$ from Eq. (13). On the other hand, in the classical approach in the absence of h and B , the classical vector describing the spin of the magnetic impurity is *conventionally* chosen along a certain direction (the spin quantization axis). Thus, the solutions of the BdG equations, including the YSR in-gap levels, have the spin projection on the spin quantization axis as a good quantum number. This has led to the perception that the YSR excitations are indeed spin polarized in both weak and strong coupling regimes. Below, when considering the classical approach, we shall follow the same convention.

Next, we discuss the polarization function $P(\omega)$ of the YSR excitations as a function of the exchange coupling and the applied magnetic field in the single-site model and compare the results to the classical approach. As anticipated above, we will show that the presence of either the exchange or magnetic field is required for the YSR excitations to have nonzero polarization. In the absence of a magnetic field, the polarization of the states is protected by the exchange field h , which can be of the order of a few Tesla, thus, making the polarization robust against thermal fluctuations and environmental noise. Figure 3 shows the polarization spectral function $P(\omega)$ of the YSR excitations as a function of the exchange coupling J for the finite value of the exchange field: In the absence of an external magnetic field, the single-site model predicts the existence of a pair of spin-polarized YSR excitations both in the weak and in the strong coupling limit [see Fig. 3(a)]. The polarization spectrum in the classical model shows a somewhat similar behavior: two spin-polarized YSR excitations crossing at the critical value of the exchange coupling [see Fig. 4(a)]. However, closer examination reveals a crucial difference between the two approaches: While in the classical limit, the YSR excitations are fully polarized for any value of J (see Fig. 4), in the quantum approach, the polarization of the YSR excitations at $\omega > 0$ depends on the exchange field h and coupling J as

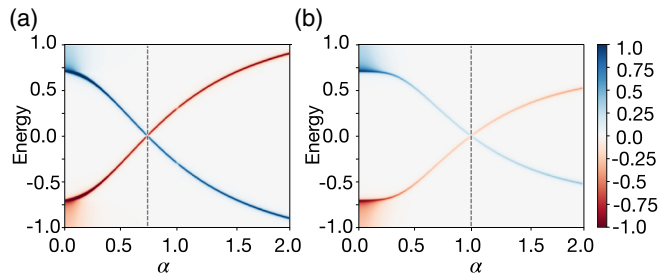


FIG. 4. Polarization of the YSR excitations from the classical approach as a function of the dimensionless coupling parameter $\alpha \simeq JS$ for two different impurity-spin S orientations: parallel (a) and perpendicular (b) to the exchange field h . In order to highlight the polarization of the YSR excitations here we plot $A_{\uparrow}(\omega) - A_{\downarrow}(\omega)$ normalized by the maximum value of the total density of states, that eliminates contribution from the continuum of states. The dashed line indicates the phase transition. The energies are in units of the superconducting pairing potential Δ . In the two panels, we have set $h = 0.3$.

follows:

$$\frac{Z_{\uparrow} - Z_{\downarrow}}{Z_{\uparrow} + Z_{\downarrow}} \propto \frac{\gamma_0^2 - 1}{\gamma_0^2 + 1} = \frac{h}{\sqrt{h^2 + J^2}}. \quad (14)$$

Thus, at a finite value of h , the YSR excitations are polarized even for $B = 0$. Applying an external magnetic field alters the polarization of the YSR excitations. In the presence of the magnetic field, one of the ground states in the weak coupling regime (or a linear combination of them) is selected and the system is no longer described by a mixed state, which further enhances the polarization.

Regarding the effects of the external magnetic field, we first consider the case when $\mathbf{B} \parallel \mathbf{h}$ in Fig. 3(b). In the weak coupling regime, the system exhibits a pair of fully polarized YSR excitations and a similar result is obtained using the classical approach. However, in the strong coupling regime applying the magnetic field splits the YSR excitations into two pairs of the subgap excitations: the main YSR state and its “satellite” with lower polarization [see Fig. 3(b) for $J > J_c$]. For $\mathbf{B} \parallel \mathbf{h}$ the polarization of the satellite state behaves as $P(\omega) \propto -\gamma^2$, where $\gamma = [B + 2h + \sqrt{(B + 2h)^2 + 4J^2}]/2J$, and it has the opposite sign compared to the main YSR state spin orientation. For the details of the polarization calculations see Appendix B.

Changing the orientation of the external magnetic field allows us to control the polarization of the pair of subgap excitations as shown in Fig. 3(c): By applying the magnetic field perpendicularly to the direction of the exchange field reverses the spin polarization of the satellite peaks, such that two states have the same polarization orientation. For $\mathbf{B} \perp \mathbf{h}$ the polarization of both the main YSR peaks and their satellites decreases with increasing exchange coupling J .

To summarize, an external magnetic field can be used as a knob for tuning the spin polarization of the YSR excitations. Figure 5 shows the polarization of the YSR excitations as a function of the angle subtended by the applied magnetic and exchange fields $\theta \in (0, \pi)$. In the single-site approach, the behavior of polarization depends on the strength of the exchange coupling: in the weak coupling regime, the spin polarization

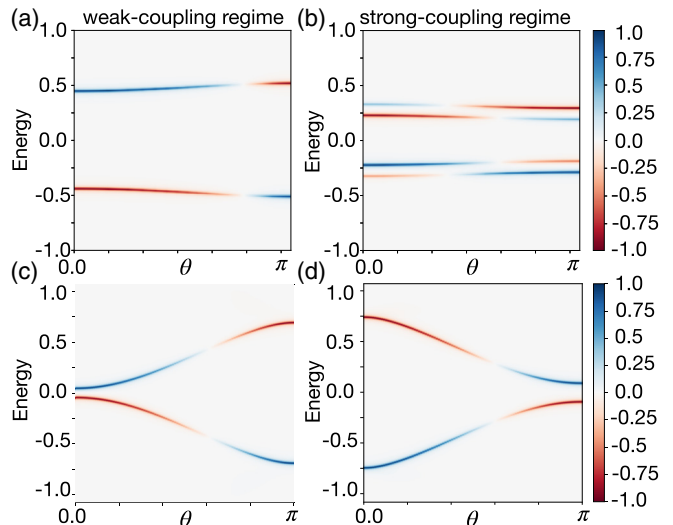


FIG. 5. Polarization spectral density as a function of the energy E and the angle of the external magnetic field $\mathbf{B} = B(\cos \theta, \sin \theta)$ in the weak and strong coupling regime for the single-site (a, b) and classical (c, d) approaches. Energies are given in units of Δ . The choice of system parameters is $B = 0.1, h = 0.3$.

of the YSR excitations switches with θ , while in the strong coupling regime, due to the splitting of the YSR excitations in the magnetic field, the response is qualitatively different: The switching happens between the main YSR state and its satellite. Additionally, the switching of polarization occurs at different values of θ for the YSR state and its satellite. Thus, there is a range of θ around $\pi/2$ for which there is a pair states with the same finite spin polarization. On the other hand, as mentioned above, in the classical case, there is no qualitative difference in the polarization behavior between the strong and weak coupling regimes.

IV. CONCLUSIONS

We have studied a system consisting of a ferromagnetic insulator/superconductor structure coupled to a quantum dot in the Kondo regime. We demonstrate that the spin splitting induced in the superconductor via the magnetic proximity effect leads to spin polarization of the YSR excitations even in the absence of an external magnetic field.

To capture the quantum nature of the quantum dot spin in a qualitative fashion, we employed a single-site model describing a quantum impurity coupled to a spin-split single-site superconductor. This model, despite its simplicity, correctly captures the many-body nature of the system’s ground state, in particular, the QPT occurring as a function of the exchange coupling, accompanied by the change in the fermion parity and the total spin of the ground state. Both the weak and the strong coupling phases are characterized by the low-energy spin-polarized YSR excitations. The exchange coupling strength can be adjusted in tunneling experiments through manipulation of the distance between the sample and the tip [43], or in quantum-dot experiments by applying a gate voltage to the quantum dot [14]. This allows for exploration of the range from weak to strong exchange coupling regimes.

We find that the single-site model predicts the splitting of the YSR excitations in the strong coupling regime, while the classical impurity limit does not describe this splitting. Changing the orientation of the magnetic field allows controlling the polarization of the YSR excitations, namely, rotation of the magnetic field allows us to switch the polarization of the excitations.

To go beyond the qualitative picture provided by the single-site model, one has to perform the NRG calculations similar to Ref. [27]. The NRG method can give a quantitative description of the quantum phase transition, of the splitting of the YSR states in the magnetic field. However, for the system studied here we do not expect the NRG spectra to differ *qualitatively* from the ones obtained using the single-site model.

For applications in spintronics and transport in quantum devices, the main advantage of using an FMI is that the polarization of the YSR excitations occurs without the need of applying a large external magnetic field which would inevitably affect superconductivity. The results of our paper can have implications for the physics of transmon devices that have been recently realized in a semiconducting-superconducting nanowires coupled to a quantum dot [15,16]. Our results can be straightforwardly extended to other setups, as for example molecules on the surface of superconductors with larger spin number, magnetic anisotropy, as well as anisotropic exchange coupling [24,35].

Note added. Recently, we become aware that a spin splitting in the even parity sector in the absence of an external magnetic field can be induced when going beyond the single-site model. This effect enhances the robustness of the polarization of the YSR. A detailed calculation will be reported in a separate publication.

ACKNOWLEDGMENTS

A.S., D.B., and M.A.C. acknowledge the support from the Spanish MICINN-AEI through Project No. PID2020-120614GB-I00 (ENACT) and the funding from the Basque Government's IKUR initiative on Quantum technologies (Department of Education). F.S.B. acknowledges the support from the Spanish MICINN-AEI through Projects No. PID2020-114252GB-I00 (SPIRIT) and No. TED2021-130292B-C42, the Basque Government through Grant No. IT-1591-22, and the EU's Horizon 2020 Research and Innovation Program under Grant No. 800923 (SUPERTED). D.B. acknowledges the Transnational Common Laboratory Quantum-ChemPhys.

APPENDIX A: CLASSICAL APPROACH

Following Yu's, Shiba's, and Rusinov's [1–3] original works, the problem of a classical impurity on a superconductor can be analytically solved by accounting for the exchange field in the bare superconductor GF. To this end, notice that the BdG Hamiltonian describing a spin-split superconductor written in the Nambu basis, i.e., $\Psi_{\mathbf{k}} = (c_{\mathbf{k}\uparrow} c_{\mathbf{k}\downarrow} c_{-\mathbf{k}\downarrow}^\dagger - c_{-\mathbf{k}\uparrow}^\dagger)^T$, takes the form

$$H = \sum_{\mathbf{k}} \Psi_{\mathbf{k}}^\dagger H_{\mathbf{k}}^{\text{BdG}} \Psi_{\mathbf{k}},$$

$$H_{\mathbf{k}}^{\text{BdG}} = \epsilon_{\mathbf{k}} \tau_3 + \Delta \tau_1 + h \sigma_3 \tau_0, \quad (\text{A1})$$

where $\tau_{i=1,2,3}$ and $\sigma_{i=1,2,3}$ are the Pauli matrices corresponding to the particle-hole and the spin degrees of freedom, respectively. Hence, the unperturbed GF of a spin-split superconductor reads

$$\hat{G}_0^{-1}(\omega, \mathbf{k}) = i\omega\sigma_0\tau_0 - H_{\mathbf{k}}^{\text{BdG}},$$

$$\hat{G}_0(\omega, \mathbf{k}) = \frac{(h - \omega)\tau_0 - \xi_{\mathbf{k}}\tau_3 - \Delta\tau_1}{\Delta^2 + \xi_{\mathbf{k}} - (h - \omega)^2}. \quad (\text{A2})$$

Performing summation over the momenta, we obtain the local GF:

$$\hat{G}_0(\omega) = -\pi\nu \frac{(h - \omega)\tau_0 - \Delta\tau_1}{\sqrt{\Delta^2 - (\omega - h)^2}}, \quad (\text{A3})$$

where ν is the electron density of states at the Fermi level. The exchange coupling in the limit of classical impurity is given by a scattering potential $\hat{V} = \frac{J}{2} \mathbf{S} \cdot \boldsymbol{\sigma}$, where J is an exchange coupling between the impurity spin S and the spin density of a superconductor. Note that in the classical limit S is a vector.

We compute the T matrix, whose poles are the energies of the subgap bound states. The T matrix can be defined using the following equation for the perturbed local GF matrix:

$$\hat{G}(\omega) = \hat{G}_0(\omega) + \hat{G}_0(\omega)\hat{T}(\omega)\hat{G}_0(\omega). \quad (\text{A4})$$

Upon comparing this equation with the Dyson equation, we arrive at $\hat{T}(\omega) = \hat{V}[1 - \hat{G}_0(\omega)\hat{V}]^{-1}$. Hence, for an impurity aligned with the external magnetic field, we obtain

$$\hat{G}(\omega) = -\frac{\pi\nu}{D} \begin{pmatrix} a & \Delta \\ \Delta & a \end{pmatrix}, \quad (\text{A5})$$

with $D = 2\alpha(h - \omega) + (\alpha^2 - 1)\sqrt{\Delta^2 - (h - \omega)^2}$ and $a = h - \omega - \alpha\sqrt{\Delta^2 - (h - \omega)^2}$, where we have introduced the dimensionless parameter $\alpha = \pi\nu JS/2$. The local retarded GF $G^R(\omega)$ is obtained by replacing $\omega \rightarrow \omega + i\delta$ in the above expression, where $\delta \rightarrow 0^+$. The spin-resolved spectral function is obtained from normal components of the GF matrix using

$$A_{\sigma=\{\uparrow,\downarrow\}}^{\text{cl}}(\omega) = -\frac{1}{\pi} \text{Im}[G_{\sigma\sigma}^R(\omega)]. \quad (\text{A6})$$

For $h > 0$ $A_{\uparrow}^{\text{cl}}(\omega)$ has the YSR peak at $\omega_{\uparrow} = h - \Delta \frac{(1-\alpha^2)}{(1+\alpha^2)}$, while $A_{\downarrow}^{\text{cl}}(\omega)$ has a peak at $\omega_{\downarrow} = -h + \Delta \frac{(1-\alpha^2)}{(1+\alpha^2)}$. Notice that when the external magnetic and exchange fields are aligned this approach yields two fully spin-polarized YSR excitations. Thus, the exchange field merely introduces a shift of the the YSR peak energy. A closed analytical expression of the energy of the YSR peaks can also be obtained for \mathbf{B} perpendicular to the exchange field \mathbf{h} , but not in the general case. However, by obtaining the spin polarization numerically we observe that the main difference between the aligned and nonaligned cases is the change in the spin polarization of the YSR excitations, which changes from being fully polarized to partially polarized as the angle θ between the magnetic and exchange field increases.

APPENDIX B: SPIN POLARIZATION OF THE YSR EXCITATIONS IN THE SINGLE-SITE MODEL

In this Appendix, we calculate spin polarization of the YSR excitations in the single-site approximation. Assuming

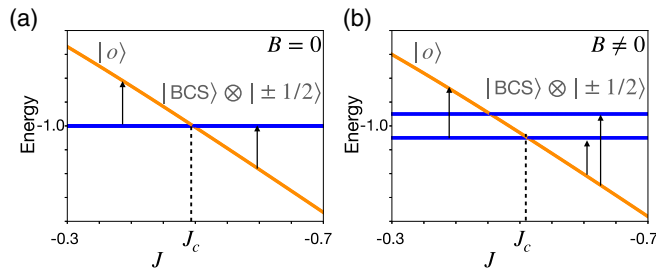


FIG. 6. Schematic representation of the low-energy spectrum of the single-site model as a function of exchange coupling J for the case of zero (a) and nonzero (b) magnetic field B . Arrows indicate possible transitions in the weak coupling ($J < J_c$) and in the strong coupling ($J > J_c$) regimes.

nonzero exchange field we obtain the polarization of the YSR excitations analytically for the cases of $B = 0$ and $\mathbf{B} \parallel \mathbf{h}$. The results are shown in Figs. 3(a) and 3(b).

When $h \neq 0$ and $B = 0$ the polarization $P(\omega)$ is computed using the expression given in Eq. (10) of the main text. The low-energy spectrum for this choice of parameters is shown in Fig. 6(a). In the weak coupling regime ($J < J_c$) the ground state at $\epsilon_0 = -\Delta$ is twofold degenerate and is described by the density matrix ρ_e in Eq. (11). The first excited state with the energy $\epsilon_1 = -\frac{h+\sqrt{h^2+J^2}}{J}$ is given by

$$|o\rangle = \frac{1}{\sqrt{1+\gamma_0^2}}(|\downarrow, 1/2\rangle - \gamma_0|\uparrow, -1/2\rangle), \quad (\text{B1})$$

where $\gamma_0 = \frac{h+\sqrt{h^2+J^2}}{J}$. The amplitudes of the spectral function are

$$\begin{aligned} Z_\uparrow &= |\langle o|c_\uparrow^\dagger|\rho_e\rangle|^2 = \frac{\gamma_0^2}{8(1+\gamma_0^2)}, \\ Z_\downarrow &= |\langle o|c_\downarrow^\dagger|\rho_e\rangle|^2 = \frac{1}{8(1+\gamma_0^2)}. \end{aligned} \quad (\text{B2})$$

In this case, there is a single spin-polarized YSR excitation at $\omega = \epsilon_1 - \epsilon_0$ and its polarization is given by

$$P(\omega) = \left(\frac{\gamma_0^2 - 1}{1 + \gamma_0^2} \right) \delta(\omega - \epsilon_1 + \epsilon_0), \quad (\text{B3})$$

with the amplitude decreasing as a function of the exchange coupling as $\frac{\gamma_0^2 - 1}{1 + \gamma_0^2} \propto \frac{h}{\sqrt{h^2 + J^2}}$ for a fixed value of the exchange field. When $h \neq 0$ and $\mathbf{B} \parallel \mathbf{h}$ low-energy states involved in the YSR excitations are shown in Fig. 6(b). Let us discuss the weak and strong coupling regimes separately. For $J < J_c$ the

magnetic field selects (with probability $p_- = 1$) one of the doublet parity-even states $|e_-\rangle$ as the absolute ground state. The first excited parity-odd state $|o\rangle$ is as in Eq. (B1) but with $\gamma = \frac{(B+2h+\sqrt{(B+2h)^2+4J^2})}{2J}$. Hence, the spectral weights for spin excitations are the following:

$$\begin{aligned} Z_\uparrow &= |\langle o|c_\uparrow^\dagger|e_-\rangle|^2 = \frac{\gamma^2}{2(1+\gamma^2)}, \\ Z_\downarrow &= |\langle o|c_\downarrow^\dagger|e_-\rangle|^2 = 0. \end{aligned} \quad (\text{B4})$$

Therefore, in the weak coupling regime, there is a single YSR peak with constant polarization intensity $P(\omega) \propto (Z_\uparrow - Z_\downarrow)/(Z_\uparrow + Z_\downarrow) = 1$. The strong coupling regime requires more care. For $J > J_c$ the ground state is given by the odd-parity singlet $|o\rangle$ and there are two even-parity states $|e_\pm\rangle$ the electron can tunnel to. The polarization in this case has two contributions:

$$P(\omega) = \frac{\sum_{i=\pm} (Z_\uparrow^i - Z_\downarrow^i) \delta(\omega - \epsilon_i + \epsilon_0)}{\max[Z_\uparrow^+ + Z_\downarrow^+, Z_\uparrow^- + Z_\downarrow^-]}, \quad (\text{B5})$$

where $\epsilon_{i=\pm} = -\Delta \pm \frac{B}{2}$. The spectral weights are

$$\begin{aligned} Z_\uparrow^- &= |\langle e_-|c_\uparrow^\dagger|o\rangle|^2 = 0, \\ Z_\downarrow^- &= |\langle e_-|c_\downarrow^\dagger|o\rangle|^2 = \frac{\gamma^2}{2(1+\gamma^2)}, \\ Z_\uparrow^+ &= |\langle e_+|c_\uparrow^\dagger|o\rangle|^2 = \frac{1}{2(1+\gamma^2)}, \\ Z_\downarrow^+ &= |\langle e_+|c_\downarrow^\dagger|o\rangle|^2 = 0. \end{aligned} \quad (\text{B6})$$

The polarization is given by the sum $P(\omega) = P_+(\omega) + P_-(\omega)$ with

$$\begin{aligned} P_+(\omega) &= \frac{Z_\uparrow^+}{Z_\uparrow^+} \delta(\omega - \epsilon_+ + \epsilon_0), \\ P_-(\omega) &= -\frac{Z_\downarrow^-}{Z_\uparrow^+} \delta(\omega - \epsilon_- + \epsilon_0), \end{aligned} \quad (\text{B7})$$

where we normalize each term by Z_\uparrow^+ , because $Z_\uparrow^+ > Z_\downarrow^-$ for $J > J_c$. Two components $P_\pm(\omega)$ correspond to the main YSR excitation and its satellite, respectively. These two states show different behavior as a function of the exchange coupling J : the polarization intensity of the satellite state $P_- \propto -\gamma^2$ with $\gamma = \frac{B+2h}{\sqrt{(B+2h)^2+4J^2}}$ increases as a function of J , while the polarization of the main YSR excitation $P_+(\omega)$ stays constant as a function of J and has an opposite spin orientation.

- [1] Yu. Luh, Bound state in superconductors with paramagnetic impurities, *Acta Phys. Sin.* **21**, 75 (1965).
- [2] H. Shiba, Classical spins in superconductors, *Prog. Theor. Phys.* **40**, 435 (1968).
- [3] A. I. Rusinov, On the theory of gapless superconductivity in alloys containing paramagnetic impurities, *Sov. J. Exp. Theor. Phys.* **29**, 1101 (1969).

- [4] A. Yazdani, B. A. Jones, C. P. Lutz, M. F. Crommie, and D. M. Eigler, Probing the local effects of magnetic impurities on superconductivity, *Science* **275**, 1767 (1997).
- [5] S.-H. Ji, T. Zhang, Y.-S. Fu, X. Chen, X.-C. Ma, J. Li, W.-H. Duan, J.-F. Jia, and Q.-K. Xue, High-Resolution Scanning Tunneling Spectroscopy of Magnetic Impurity Induced Bound

- States in the Superconducting Gap of Pb Thin Films, *Phys. Rev. Lett.* **100**, 226801 (2008).
- [6] B. W. Heinrich, J. I. Pascual, and K. J. Franke, Single magnetic adsorbates on *s*-wave superconductors, *Prog. Surf. Sci.* **93**, 1 (2018).
- [7] V. Kaladzhyan, C. Bena, and P. Simon, Characterizing *p*-wave superconductivity using the spin structure of Shiba states, *Phys. Rev. B* **93**, 214514 (2016).
- [8] J. Ortuzar, S. Trivini, M. Alvarado, M. Rouco, J. Zaldivar, A. L. Yeyati, J. I. Pascual, and F. S. Bergeret, Yu-Shiba-Rusinov states in two-dimensional superconductors with arbitrary Fermi contours, *Phys. Rev. B* **105**, 245403 (2022).
- [9] M. Uldemolins, A. Mesaros, and P. Simon, Quasiparticle focusing of bound states in two-dimensional *s*-wave superconductors, *Phys. Rev. B* **105**, 144503 (2022).
- [10] J. O. Island, R. Gaudenzi, J. de Bruijkere, E. Burzurí, C. Franco, M. Mas-Torrent, C. Rovira, J. Veciana, T. M. Klapwijk, R. Aguado, and H. S. J. van der Zant, Proximity-Induced Shiba States in a Molecular Junction, *Phys. Rev. Lett.* **118**, 117001 (2017).
- [11] R. Žitko, J. S. Lim, R. López, and R. Aguado, Shiba states and zero-bias anomalies in the hybrid normal-superconductor anderson model, *Phys. Rev. B* **91**, 045441 (2015).
- [12] A. Jellinggaard, K. Grove-Rasmussen, M. H. Madsen, and J. Nygård, Tuning Yu-Shiba-Rusinov states in a quantum dot, *Phys. Rev. B* **94**, 064520 (2016).
- [13] M. Valentini, F. Peñaranda, A. Hofmann, M. Brauns, R. Hauschild, P. Krogstrup, P. San-Jose, E. Prada, R. Aguado, and G. Katsaros, Nontopological zero-bias peaks in full-shell nanowires induced by flux-tunable Andreev states, *Science* **373**, 82 (2021).
- [14] E. J. Lee, X. Jiang, M. Houzet, R. Aguado, C. M. Lieber, and S. De Franceschi, Spin-resolved Andreev levels and parity crossings in hybrid superconductor–semiconductor nanostructures, *Nat. Nanotechnol.* **9**, 79 (2014).
- [15] M. Pita-Vidal, A. Bargerbos, R. Žitko, L. J. Splitthoff, L. Grünhaupt, J. J. Wesdorp, Y. Liu, L. P. Kouwenhoven, R. Aguado, B. van Heck *et al.*, Direct manipulation of a superconducting spin qubit strongly coupled to a transmon qubit, *Nat. Phys.* (2023), doi: 10.1038/s41567-023-02071-x.
- [16] A. Bargerbos, M. Pita-Vidal, R. Žitko, L. J. Splitthoff, L. Grünhaupt, J. J. Wesdorp, Y. Liu, L. P. Kouwenhoven, R. Aguado, C. K. Andersen *et al.*, Spectroscopy of spin-split Andreev levels in a quantum dot with superconducting leads, [arXiv:2208.09314](https://arxiv.org/abs/2208.09314).
- [17] A. V. Balatsky, I. Vekhter, and J.-X. Zhu, Impurity-induced states in conventional and unconventional superconductors, *Rev. Mod. Phys.* **78**, 373 (2006).
- [18] A. Villas, R. L. Klees, G. Morrás, H. Huang, C. R. Ast, G. Rastelli, W. Belzig, and J. C. Cuevas, Tunneling processes between Yu-Shiba-Rusinov bound states, *Phys. Rev. B* **103**, 155407 (2021).
- [19] L. Schneider, P. Beck, J. Wiebe, and R. Wiesendanger, Atomic-scale spin-polarization maps using functionalized superconducting probes, *Sci. Adv.* **7**, eabd7302 (2021).
- [20] H. Huang, J. Senkiel, C. Padurariu, R. Drost, A. Villas, R. L. Klees, A. L. Yeyati, J. C. Cuevas, B. Kubala, J. Ankerhold, K. Kern, and C. R. Ast, Spin-dependent tunneling between individual superconducting bound states, *Phys. Rev. Res.* **3**, L032008 (2021).
- [21] M. Ruby, Y. Peng, F. von Oppen, B. W. Heinrich, and K. J. Franke, Orbital Picture of Yu-Shiba-Rusinov Multiplets, *Phys. Rev. Lett.* **117**, 186801 (2016).
- [22] D.-J. Choi, C. Rubio-Verdú, J. De Bruijkere, M. M. Ugeda, N. Lorente, and J. I. Pascual, Mapping the orbital structure of impurity bound states in a superconductor, *Nat. Commun.* **8**, 1 (2017).
- [23] T. Machida, Y. Nagai, and T. Hanaguri, Zeeman effects on Yu-Shiba-Rusinov states, *Phys. Rev. Res.* **4**, 033182 (2022).
- [24] F. von Oppen and K. J. Franke, Yu-Shiba-Rusinov states in real metals, *Phys. Rev. B* **103**, 205424 (2021).
- [25] H. Schmid, J. F. Steiner, K. J. Franke, and F. von Oppen, Quantum Yu-Shiba-Rusinov dimers, *Phys. Rev. B* **105**, 235406 (2022).
- [26] D. Wang, J. Wiebe, R. Zhong, G. Gu, and R. Wiesendanger, Spin-Polarized Yu-Shiba-Rusinov States in an Iron-Based Superconductor, *Phys. Rev. Lett.* **126**, 076802 (2021).
- [27] W.-V. van Gerven Oei, D. Tanasković, and R. Žitko, Magnetic impurities in spin-split superconductors, *Phys. Rev. B* **95**, 085115 (2017).
- [28] X. Hao, J. S. Moodera, and R. Meservey, Thin-Film Superconductor in an Exchange Field, *Phys. Rev. Lett.* **67**, 1342 (1991).
- [29] R. Meservey and P. Tedrow, Spin-polarized electron tunneling, *Phys. Rep.* **238**, 173 (1994).
- [30] E. Strambini, V. N. Golovach, G. De Simoni, J. S. Moodera, F. S. Bergeret, and F. Giazotto, Revealing the magnetic proximity effect in EuS/Al bilayers through superconducting tunneling spectroscopy, *Phys. Rev. Mater.* **1**, 054402 (2017).
- [31] A. Hijano, S. Ilić, M. Rouco, C. González-Orellana, M. Ilyn, C. Rogero, P. Virtanen, T. T. Heikkilä, S. Khorshidian, M. Spies, N. Ligato, F. Giazotto, E. Strambini, and F. S. Bergeret, Coexistence of superconductivity and spin-splitting fields in superconductor/ferromagnetic insulator bilayers of arbitrary thickness, *Phys. Rev. Res.* **3**, 023131 (2021).
- [32] T. Tokuyasu, J. A. Sauls, and D. Rainer, Proximity effect of a ferromagnetic insulator in contact with a superconductor, *Phys. Rev. B* **38**, 8823 (1988).
- [33] T. T. Heikkilä, M. Silaev, P. Virtanen, and F. S. Bergeret, Thermal, electric and spin transport in superconductor/ferromagnetic-insulator structures, *Prog. Surf. Sci.* **94**, 100540 (2019).
- [34] E. Vecino, A. Martín-Rodero, and A. L. Yeyati, Josephson current through a correlated quantum level: Andreev states and π junction behavior, *Phys. Rev. B* **68**, 035105 (2003).
- [35] S. Trivini, J. Ortuzar, K. Vaxevani, J. Li, F. S. Bergeret, M. A. Cazalilla, and J. I. Pascual, Pair excitations of a quantum spin on a proximitized superconductor, Cooper Pair Excitation Mediated by a Molecular Quantum Spin on a Superconducting Proximitized Gold Film, *Phys. Rev. Lett.* **130**, 136004 (2023).
- [36] R. Bulla, T. A. Costi, and T. Pruschke, Numerical renormalization group method for quantum impurity systems, *Rev. Mod. Phys.* **80**, 395 (2008).
- [37] S. Vaitiekėnas, Y. Liu, P. Krogstrup, and C. Marcus, Zero-bias peaks at zero magnetic field in ferromagnetic hybrid nanowires, *Nat. Phys.* **17**, 43 (2021).
- [38] In contrast to Ref. [34], for the quantum dot setup of Fig. 1, we consider here only the Kondo regime in which the dot is singly occupied.
- [39] R. Wiesendanger, Spin mapping at the nanoscale and atomic scale, *Rev. Mod. Phys.* **81**, 1495 (2009).

- [40] P. Coleman, *Introduction to Many-Body Physics* (Cambridge University, New York, 2015).
- [41] G. D. Mahan, *Many Particle Physics*, 3rd ed. (Plenum, New York, 2000).
- [42] Since we assume a particle-hole symmetric version of the impurity model (i.e., no scattering potential), the $\omega < 0$ part of $A_\sigma(\omega)$ can be simply obtained by the replacement with $\omega \rightarrow -\omega$.
- [43] S. Karan, H. Huang, A. Ivanovic, C. Padurariu, B. Kubala, K. Kern, J. Ankerhold, and C. R. Ast, Tracking a spin-polarized superconducting bound state across a quantum phase transition, [arXiv:2304.02955](https://arxiv.org/abs/2304.02955).